



# Dynamic Nuclear Polarization

Dr. Matthew E. Merritt, Assistant Professor, Advanced Imaging Research Center, Southwestern Medical Center at Dallas



Dynamic Nuclear Polarization (DNP) is a phenomenon by which high spin polarization, typically derived from a bath of free radical electrons, is transferred to a nuclear spin bath, enhancing the difference between the nuclear energy levels and thereby producing dramatically enhanced NMR signals for detection. The phenomenon was first predicted by Overhauser,<sup>1</sup> but was not observed experimentally until the work of Slichter in metals in 1953.<sup>2</sup> It was soon

understood that the same technique could be used to develop high polarizations of <sup>1</sup>H, <sup>2</sup>H, and <sup>13</sup>C in non-conducting solids. This advance became foundational for production of solid targets for high energy physics research.<sup>3-5</sup> High nuclear polarizations in the targets simplified the results of neutron scattering experiments. Subsequently, the DNP method migrated to chemistry, being used to study a variety of structural questions in the solid state.<sup>6,7</sup> Robert Griffin of MIT has pioneered the use of DNP for signal enhancement in solid state NMR distance measurements for structural biology.<sup>8</sup> In his method, a water soluble free radical is doped into a matrix containing H<sub>2</sub>O/glycerol and the solute molecule/protein to be studied. This method has recently been used to study the K intermediate of bacteriorhodopsin in intact purple membrane.<sup>9</sup> While DNP is also possible in the liquid state, it is much less efficient due to the diminishment of the intermolecular dipolar couplings by fast molecular tumbling.<sup>10</sup>

The production of hyperpolarized molecular imaging agents has sparked great enthusiasm in the MRI community due to its potential application as a clinically viable method for assessing *in vivo* metabolism. Golman and co-workers demonstrated that a hyperpolarized solid may be rapidly melted with a bolus of boiling water and shuttled out of the DNP system using high pressure helium gas.<sup>11</sup> The hyperpolarized solute molecule can be used as an imaging agent<sup>12-14</sup>. The most popular molecule to date for hyperpolarization studies has been [1-<sup>13</sup>C]pyruvate, though other common metabolites have also been used successfully. This technique now stands as one of the most promising new methods for measuring *in vivo* metabolism.

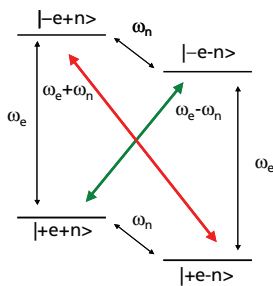


**Figure 1.** Energy level diagram for a coupled electron-nuclear spin system. The normally forbidden transitions (colored arrows) can be excited by microwave irradiation, resulting in dramatically increased nuclear polarizations.

## Dynamic Nuclear Polarization

The DNP phenomenon was first recognized as theoretically possible as an outflow of basic research into the nature of cross relaxation in NMR. Figure 1 shows the energy level diagram for a single electron

coupled to a nuclear spin in a strong magnetic field. The gyromagnetic ratio for an electron spin is ~2400 times greater than that of a <sup>13</sup>C nucleus. Therefore the single quantum transitions associated with the electrons are in the gigahertz regime (94 GHz at 3.35T) while the carbon Larmor frequency is ~35 MHz. Normally, zero (Figure 1 red arrow) or double quantum transitions (Figure 1 green arrow) are strictly forbidden. However, the hyperfine coupling between the spins is of sufficient magnitude that the 4 energy levels are not pure states, and consequently these transitions become partially allowed. Under microwave irradiation at the electron resonance frequency ± the nuclear frequency these transitions are stimulated and the nuclear polarization is enhanced in a positive or negative manner depending on the transition that is irradiated (Figure 2). This is known in the literature as the solid effect. This mechanism is active when the electron resonance has a linewidth of the same order or less than the nuclear Larmor frequency. This is commonly the case when the trityl radical is used for polarizing protons. However, at 3.35T the FWHM of the electron resonance is ~44 MHz.<sup>15</sup> Therefore, when using trityl and <sup>13</sup>C, the thermal mixing mechanism is likely the main source of polarization. Thermal mixing is another DNP mechanism that is active when the electron resonance is wider than the nuclear Larmor frequency, as is common when nitroxide radicals such as TEMPO are used or when lower  $\gamma$  nuclei are the targets. An excellent description of the differences between the two mechanisms is outlined in the paper by Comment, et. al.<sup>16</sup> In a somewhat simplified picture, thermal mixing is a three spin effect as opposed to two in the solid effect. It also depends upon strong dipolar couplings between electron spins, in effect, the presence of an electron spin bath that can be described with a single temperature. Irradiation of the bath at a certain frequency causes other coupled electron spins to flip. Since the spins at other resonance frequencies have slightly different energies, the difference can be made up with a coupled nuclear spin. Since a difference in frequencies is still necessary like in the solid effect, thermal mixing again produces characteristic positive and negative enhancements, though the maxima are separated by a number closer to the Larmor frequency of the nucleus (Figure 2). Traditionally, it has been understood that the solid effect required more power than thermal mixing since forbidden transitions are pumped. In thermal mixing, no forbidden transitions are present and therefore it might be expected to be a more efficient mechanism. This likely explains the extremely high polarizations achievable when using trityl and <sup>13</sup>C. New bi-radicals seek to increase the available polarization by tethering the free electrons together, resulting in stronger electron dipolar couplings and enhancing thermal mixing for protons.<sup>17</sup>

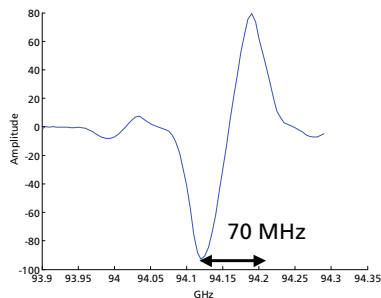


**Figure 2.** DNP enhancement curve as a function of frequency for [1-<sup>13</sup>C]pyruvate mixed with the trityl radical. Each data point was collected after irradiation for 300 seconds, which is not long enough to reach the equilibrium polarization. The 70 MHz splitting observed would lead one to believe that the solid effect is active, but longer irradiation times show a splitting between the maxima of ~63 MHz, indicating thermal mixing as the source of enhancement.



### Fast Dissolution DNP

The DNP method developed by Golman and co-workers has several essential elements that allow the spectacular signal enhancements seen to date.<sup>11</sup> First, the experiment is carried out at 1.2 to 1.4 K. At room temperature, the enhancement from DNP goes as the ratio of the gyromagnetic ratios of the dipolar coupled spins. At these very low temperatures, the Boltzmann distribution begins to display exponential behavior; at 1.4 K the electrons are ~92% polarized as opposed to less than 1% for <sup>1</sup>H and <sup>13</sup>C. Consequently, DNP at low temperatures can produce nuclear polarizations in the percent range as well, which is far greater than the enhancement available at room temperature. The second, key insight was the realization that the sample could be melted on a time scale fast enough that large polarizations were left over after the dissolution. The developed polarization decays with the normal T<sub>1</sub> of the nucleus. If the melting is slow, sufficient sensitivity is not retained in the experiment. Typically, melting of a 40 to 200 μl DNP sample is accomplished with 3 ml–6 ml of water at ~190 °C and 10 bar of pressure supplied by a compressed helium tank. Due to the constraints imposed by the decay of the magnetization, protonated carbons are typically more difficult to use for DNP. C-1 labeled pyruvate has been a metabolite of choice since the C-3 protons are distal from the observed carbon. Hence, the primary source of relaxation arises from the chemical shift anisotropy. The T<sub>1</sub> of the C-1 carbon of pyruvate is close to 1 minute at 1.5 Tesla and ~40 seconds at 14.1 T.

### Metabolism using Hyperpolarization Technique

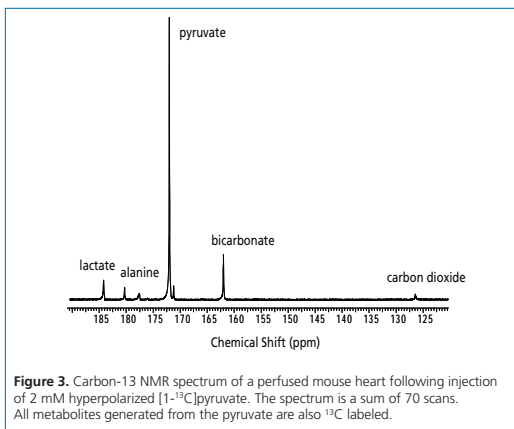


**Figure 3.** Carbon-13 NMR spectrum of a perfused mouse heart following injection of 2 mM hyperpolarized [1-<sup>13</sup>C]pyruvate. The spectrum is a sum of 70 scans. All metabolites generated from the pyruvate are also <sup>13</sup>C labeled.

The central feature that makes imaging or spectroscopy using hyperpolarized <sup>13</sup>C labeled compounds so appealing is the incredible gains in signal to noise that can be achieved, allowing observation of biochemical reactions *in vivo* and *in vitro* that previously could not be monitored with any technique (Figure 3). The most common example, hyperpolarized [1-<sup>13</sup>C]pyruvate illustrates the high information content of MR combined with hyperpolarization in powerful fashion. Figure 4 shows the information available by three different methods for assessing metabolism. Assume that three different samples have been prepared, a <sup>11</sup>C labeled pyruvate, [3-<sup>13</sup>C]pyruvate, and hyperpolarized [1-<sup>13</sup>C]pyruvate, for injection into a commonly used model of metabolism, the perfused rat heart. Observation of the <sup>11</sup>C compound by positron emission tomography (PET) will reveal only the uptake of the pyruvate, producing the familiar dose-response curve (Figure 4, A). Observation of the delivery of the [3-<sup>13</sup>C]pyruvate by NMR would allow not only the uptake of the pyruvate to be monitored, but also its subsequent metabolism to lactate and alanine. It has been shown that detection of the label using indirect methods such as heteronuclear multiple quantum coherence (HMQC) can allow time points to be taken

approximately every 10–20 seconds (Figure 4, B).<sup>18</sup> The bottom panel shows the data that would be obtained following injection of the hyperpolarized substrate (Figure 4, C). Due to the increase in signal to noise, time points can be taken every second, or even faster. Also, since direct detection of the <sup>13</sup>C label is possible, flux into CO<sub>2</sub> and bicarbonate is detectable as well. In this lab, the signal to noise gain for the hyperpolarization experiment versus the HMQC method is approximately 50 times, with the bonus of much higher resolution as a function of time following the injection. The power of this technique has already been taken advantage of to study a variety of questions with physiological and pathological significance. Hyperpolarized H<sup>13</sup>CO<sub>3</sub><sup>-</sup> has been used as a means of assessing pH

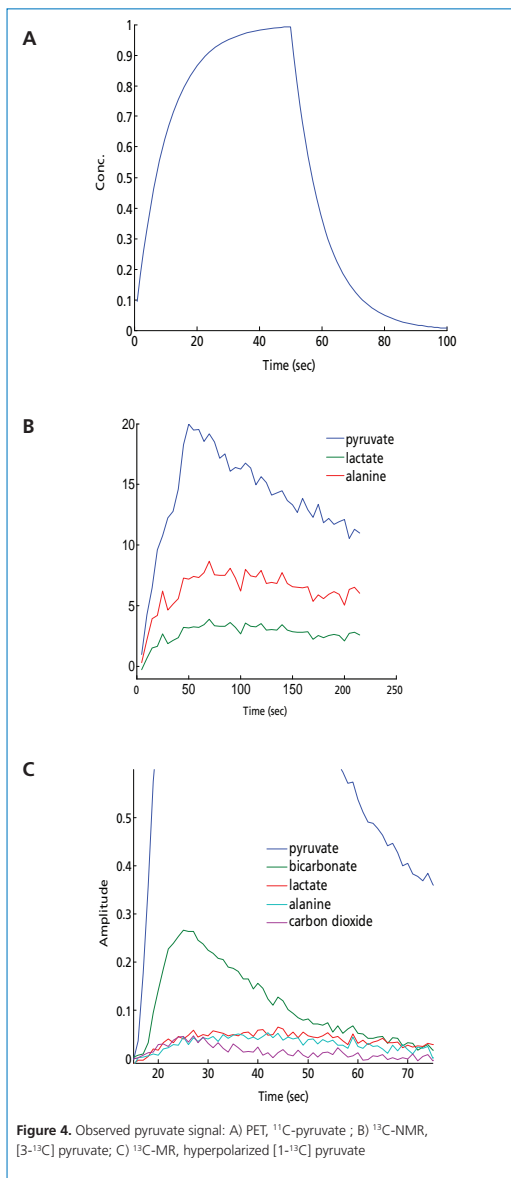


**Figure 4.** Observed pyruvate signal: A) PET, <sup>11</sup>C-pyruvate; B) <sup>13</sup>C-NMR, [3-<sup>13</sup>C] pyruvate; C) <sup>13</sup>C-MR, hyperpolarized [1-<sup>13</sup>C] pyruvate

by monitoring the equilibrium between CO<sub>2</sub> and bicarbonate.<sup>19</sup> This method of pH measurement has the unique advantage of injecting a completely benign compound as the sensor. Hyperpolarized [<sup>1-<sup>13</sup>C</sup>]pyruvate has been used to measure substrate preference in a perfused heart model, demonstrating the ability to assess flux through a single enzyme catalyzed reaction.<sup>20</sup> Workers at Cambridge University and UCSF have already shown that the kinetics of dispersal of hyperpolarized pyruvate is sensitive to cancer *in vivo*.<sup>21–23</sup> Cardiac dysfunction following myocardial infarction could also potentially be detected with this method.<sup>24,25</sup>

## Conclusion

In summary, hyperpolarization of <sup>13</sup>C compounds is an extremely promising new avenue for molecular imaging and metabolism studies. Applications to cancer and cardiac metabolism are currently under development. Clinically relevant measures of metabolism with this technique should become available during the next decade.

## References

- Overhauser, A. W. *Polarization of Nuclei in Metals*. *Physical Review* **1953**, *92*(2), 411–415.
- Carver, T. R.; Slichter, C. P. *Polarization of Nuclear Spins in Metals*. *Physical Review* **1953**, *92*(1), 212–213.
- Abraham, A.; Goldman, M. *Nuclear Magnetism: Order and Disorder*. Oxford: Oxford University Press; **1982**, 625 p.
- de Boer, W. *Dynamic orientation of nuclei at low temperatures*. *Journal of Low Temperature Physics* **1976**, *22*(1), 185–212.
- de Boer, W.; Borghini, M.; Morimoto, K.; Niinikoski, T. O.; Udo, F. *Dynamic Polarization of Protons, Deuterons, and Carbon-13 Nuclei: Thermal Contact Between Nuclear Spins and an Electron Spin-Spin Interaction Reservoir*. *Journal of Low Temperature Physics* **1974**, *15*(3–4), 249–267.
- Afeworki, M.; McKay, R. A.; Schaefer, J. *Selective observation of the interface of heterogeneous polycarbonate/polystyrene blends by dynamic nuclear polarization carbon-13 NMR spectroscopy*. *Macromolecules* **1992**, *25*(16), 4084–4091.
- Wind, R. A.; Duijvestijn, M. J.; Van der Lugt, C.; Manenschijs, A.; Vriend, J. *Applications of dynamic nuclear polarization in carbon-13 NMR in solids*. *Progress in Nuclear Magnetic Resonance Spectroscopy* **1985**, *17*(1), 33–67.
- Gerfen, G. J.; Becerra, L. R.; Hall, D. A.; Griffin, R. G.; Temkin, R. J.; Singel, D. J. *High frequency (140 GHz) dynamic nuclear polarization: Polarization transfer to a solute in frozen aqueous solution*. *Journal of Chemical Physics* **1995**, *102*(24), 9494.
- Mak-Jurkauskas, M. L.; Bajaj, V. S.; Hornstein, M. K.; Belenky, M.; Griffin, R. G.; Hertzfeld, J. *Energy transformations early in the bacteriorhodopsin photocycle revealed by DNP-enhanced solid-state NMR*. *Proceedings of the National Academy of Sciences* **2008**, *105*(3), 883–888.
- Loening, N. M.; Rosay, M.; Weis, V.; Griffin, R. G. *Solution-State Dynamic Nuclear Polarization at High Magnetic Field*. *Journal of the American Chemical Society* **2002**, *124*(30), 8808–8809.
- Ardenkjaer-Larsen, J. H.; Fridlund, B.; Gram, A.; Hansson, G.; Hansson, L.; Lerche, M. H.; Servin, R.; Thaning, M.; Golman, K.; *Increase in signal-to-noise ratio of > 10,000 times in liquid-state NMR*. *Proceedings of the National Academy of Sciences of the United States of America* **2003**, *100*(18), 10158–10163.
- Golman, K.; In't Zandt, R.; Lerche, M. H.; Pehrsen, R.; Ardenkjaer-Larsen, J. H.; *Metabolic imaging by hyperpolarized <sup>13</sup>C magnetic resonance imaging for *in vivo* tumor diagnosis*. *Cancer Research* **2006**, *66*(22), 10855–10860.
- Golman, K.; In't Zandt, R.; Thaning, M. *Real Time Metabolic Imaging*. *Proceedings of the National Academy of Sciences of the United States of America* **2006**, *103*(30), 11270–11275.
- Golman, K.; Petersson, J. S. *Metabolic imaging and other applications of hyperpolarized <sup>13</sup>C*. *Academic Radiology* **2006**, *13*:932–942.
- Wolber, J.; Ellner, F.; Fridlund, B.; Gram, A.; Jóhannesson, H.; Hansson, G.; Hansson, L. H.; Lerche, M. H.; Månsson, S.; Servin, R.; Thaning, M.; Golman, K.; Ardenkjaer-Larsen, J. H. *Nuclear Instruments and Methods in Physics Research Section A: Accelerators, Spectrometers, Detectors and Associated Equipment* **2004**, *526*, 173–181.
- Comment, A.; van den Brandt, B.; Uffmann, F.; Kurdzesau, F.; Jannin, S.; Konter, J. A.; Hautle, P.; Wenckebach, W. T.; Gruetter, R.; van der Klink, J. J. *Design and performance of a DNP prepolarizer coupled to a rodent MRI scanner*. *Concepts in Magnetic Resonance Part B: Magnetic Resonance Engineering* **2007**, *31B*(4), 255–269.
- Hu, K. N.; Yu, H. H.; Swager, T. M.; Griffin, R. G. *Dynamic Nuclear Polarization with Biradicals*. *J Am Chem Soc* **2004**, *126*(35), 10844–10845.
- Burgess SC, Babcock EE, Jeffrey FMH, Sherry AD, Malloy CR. *NMR indirect detection of glutamate to measure citric acid cycle flux in the isolated perfused mouse heart*. *FEBS Letters* 2001;505(1):163-167.
- Gallagher FA, Kettunen MI, Day SE, Hu D-E, Ardenkjaer-Larsen JH, Zandt Rit, Jensen PR, Karlsson M, Golman K, Lerche MH, Brindle KM. *Magnetic resonance imaging of pH in vivo using hyperpolarized <sup>13</sup>C-labelled bicarbonate*. *Nature* 2008;453(7197):940-943.
- Merritt, M. E.; Harrison C.; Storey, C. J.; Jeffrey, F. M. H.; Sherry, A. D.; Malloy, C. R.; *Hyperpolarized <sup>13</sup>C allows a direct measure of flux through a single enzyme-catalyzed step by NMR*. *Proceedings of the National Academy of Sciences of the United States of America* **2007**, *104*(50), 19773–19777.
- Albers, M. J.; Bok, R.; Chen, A. P.; Cunningham, C. H.; Zierhut M. L.; Zhang, V. Y.; Kohler, S. J.; Tropp, J.; Hurd, R. E.; Yen, Y-F; Nelson, S. J.; Vigneron, D. B.; Kurhanewicz, J. *Hyperpolarized <sup>13</sup>C Lactate, Pyruvate, and Alanine: Noninvasive Biomarkers for Prostate Cancer Detection and Grading*. *Cancer Res* **2008**, *68*(20), 8607–8615.
- Chen, A. P.; Albers, M. J.; Cunningham, C. H.; Kohler, S. J.; Yen, Y-F; Hurd, R. E.; Tropp, J.; Bok, R.; Pauly, J. M.; Nelson, S. J.; Kurhanewicz, J.; Vigneron, D. B. *Hyperpolarized C-13 spectroscopic imaging of the TRAMP mouse at 3T - Initial experience*. *Magnetic Resonance in Medicine* **2007**, *58*(6), 1099–1106.
- Day, S. E.; Kettunen, M. I.; Gallagher, F. A.; De-En, H.; Lerche, M.; Wolber, J.; Golman, K.; Ardenkjaer-Larsen, J. H.; Brindle, K. M. *Detecting tumor response to treatment using hyperpolarized <sup>13</sup>C magnetic resonance imaging and spectroscopy*. *Nature Medicine* **2007**, *13*(11), 1382–1387.
- Golman, K.; Petersson, J. S.; Magnusson, P.; Jóhannesson, E.; Åkeson, P.; Chai, C.; Hansson, G.; Månsson, S. *Cardiac metabolism measured noninvasively by hyperpolarized <sup>13</sup>C MRI*. *Magnetic Resonance in Medicine* **2008**, *59*(5), 1005–1013.
- Merritt, M. E.; Harrison, C.; Storey, C. J.; Sherry, A. D.; Malloy, C. R. *Inhibition of carbohydrate oxidation during the first minute of reperfusion after brief ischemia: NMR detection of hyperpolarized <sup>13</sup>CO<sub>2</sub> and H<sup>13</sup>CO<sub>2</sub>*. *Magnetic Resonance in Medicine* **2008**, *60*(5), 1029–1036.